PHILOSOPHICAL TRANSACTIONS B

royalsocietypublishing.org/journal/rstb

Opinion piece

Cite this article: Ekstrom AD. 2021 Regional variation in neurovascular coupling and why we still lack a Rosetta Stone. *Phil. Trans. R. Soc. B* **376**: 20190634.
http://dx.doi.org/10.1098/rstb.2019.0634

Accepted: 11 August 2020

One contribution of 10 to a theme issue 'Key relationships between non-invasive functional neuroimaging and the underlying neuronal activity'.

Subject Areas:
behaviour, neuroscience

Keywords:
fMRI, BOLD, hippocampus, neural activity, vasculature

Author for correspondence:
Arne D. Ekstrom
e-mail: adekstrom@email.arizona.edu

Regional variation in neurovascular coupling and why we still lack a Rosetta Stone

Arne D. Ekstrom[1,2]

[1]Department of Psychology, and [2]Evelyn McKnight Brain Institute, University of Arizona, 1503 E. University Boulevard, Tucson, AZ 85721, USA

ADE, 0000-0002-6812-2368

Functional magnetic resonance imaging (fMRI) is the dominant tool in cognitive neuroscience although its relation to underlying neural activity, particularly in the human brain, remains largely unknown. A major research goal, therefore, has been to uncover a 'Rosetta Stone' providing direct translation between the blood oxygen level-dependent (BOLD) signal, the local field potential and single-neuron activity. Here, I evaluate the proposal that BOLD signal changes equate to changes in gamma-band activity, which in turn may partially relate to the spiking activity of neurons. While there is some support for this idea in sensory cortices, findings in deeper brain structures like the hippocampus instead suggest both regional and frequency-wise differences. Relatedly, I consider four important factors in linking fMRI to neural activity: interpretation of correlations between these signals, regional variability in local vasculature, distributed neural coding schemes and varying fMRI signal quality. Novel analytic fMRI techniques, such as multivariate pattern analysis (MVPA), employ the distributed patterns of voxels across a brain region to make inferences about information content rather than whether a small number of voxels go up or down relative to baseline in response to a stimulus. Although unlikely to provide a Rosetta Stone, MVPA, therefore, may represent one possible means forward for better linking BOLD signal changes to the information coded by underlying neural activity.

This article is part of the theme issue 'Key relationships between non-invasive functional neuroimaging and the underlying neuronal activity'.

1. Introduction

Functional magnetic resonance imaging (fMRI) remains one of the dominant techniques in humans for relating underlying brain activity to behaviour. Indeed, compared with all other methods currently used in humans, it conveys numerous advantages. It is non-invasive and, unlike other methods like positron emission tomography (PET), requires no injections. By contrast to other methods such as scalp encephalography (EEG) and magnetoencephalography (MEG), it has superior spatial resolution (approx. $1 \times 1 \times 1$ mm voxel size as a likely upper limit [1]), and it can successfully image deep brain structures like the thalamus and hippocampus. Finally, fMRI has gone through extensive methodological development since its first uses in cognitive neuroscience in the early 90s, and techniques for performing analyses are readily available to interested students via software and other published resources [2–4].

A lingering issue with fMRI, however, is that it is an indirect measure of underlying neural activity and its relationship to neural function still remains largely undetermined, particularly outside of sensory cortices [5]. How is it that such a fundamental issue could remain unresolved? Part of the reason for this, which I will explore here, is that blood oxygen level-dependent (BOLD) signal, which forms the basis of fMRI, is itself a heterogeneous signal [6,7]. Another reason for this impasse is that 'neural' signal is also multifaceted, and therefore

THE ROYAL SOCIETY PUBLISHING

defining exactly how these two signals relate involves some degree of approximation and simplification. Finally, experiments that directly compare BOLD with neural activity are challenging, particularly in humans, leaving an important area of linkage somewhat neglected compared with studies that employ either BOLD or electrophysiology independently.

To understand the first reason why it has been difficult to pin down a neural basis for the BOLD signal across the brain (i.e. BOLD as a multifaceted signal), it is useful first to consider how this signal comes about. The BOLD signal is based on magnetic inhomogeneities produced by differences in deoxygenated versus oxygenated haemoglobin concentrations, with deoxygenated haemoglobin concentrations increasing initially owing to transient increases in neural and glial activity and then rapidly decreasing owing to the influx of freshly oxygenated blood [6,8–10]. Changes in the ratio of deoxygenated to oxygenated haemoglobin result from several different sources and have contributions from a mixture of different factors that drive the BOLD signal observed with fMRI [11]. These include cerebral oxygen metabolism ($CMRO_2$), which refers to the utilization of oxygen by active cells, cerebral blood flow (CBF), which refers to the rate at which blood flows through vessels in the brain, and cerebral blood volume (CBV), which typically indexes expansion and contraction of vessels, particularly arterioles, in response to neural and/or behavioural events. There are a variety of different invasive and non-invasive methods for measuring $CMRO_2$, CBF and CBV, and I cover these only briefly for clarity. Techniques like optical imaging allow independent measurement of $CMRO_2$ and CBF but are restricted to non-human animal models. Near-infrared spectroscopy (NIRS) allows measurement of CBF in humans but is restricted to superficial brain areas. Calibrated fMRI allows measurement of $CMRO_2$ in humans but has drawbacks in the spatial resolution I will discuss in more detail shortly. PET can, in principle, allow measurement of all three ($CMRO_2$, CBF and CBV) but the time course and spatial resolution of PET are significant limitations.

Initially, it was thought that at least one major measurable component of the BOLD signal was $CMRO_2$ [12]. The activity of neurons and glia requires at least some oxygen utilization to restore metabolic stores via the Krebs cycle (ATP) and thus would be expected to be a major component driving the BOLD signal. While some studies suggested the possibility of observing $CMRO_2$ during the earliest phase of the BOLD signal (the initial dip) [12], the inconsistency of this signal at different field strengths, in different brain regions and even across studies has led to a focus on using calibrated fMRI to measure $CMRO_2$ [13]. Calibrated fMRI involves arterial spin labelling (ASL) to 'tag' incoming blood into the brain and therefore calculate CBF. With the addition of simultaneous BOLD, hypercapnia and pulsometry, one can calculate $CMRO_2$ using an equation that relates these variables [14,15]. Consistent with this, $CMRO_2$, when it can be measured independently using calibrated fMRI, shows a robust correlation with the activity of individual neurons [7,16].

Calibrated fMRI involves, however, poorer spatial resolution, the need to employ breath holding, and overall is used infrequently compared with BOLD fMRI, thereby limiting how readily and consistently one can measure $CMRO_2$. No work to date in humans has performed calibrated fMRI and electrophysiology in the same study, and thus their relationship in humans is unknown. Glucose and other metabolites are also critical for neural function, and shifts to anaerobic processes may render oxygen consumption, in some cases, less relevant to neural activity [11]. More readily measured signals that include both oxygen and glucose metabolism are CBF and CBV, both of which alter the balance of oxygenated and deoxygenated haemoglobin. Importantly, both CBF and CBV have strong correlates with local vasculature [17], and likely play a stronger role in BOLD signal changes observed with conventional fMRI than $CMRO_2$.

Numerous findings suggest that CBF and CBV contribute substantially more to the BOLD signal than $CMRO_2$, particularly at the field strengths most often used in conventional fMRI (1.5 T, 3 T). This is because CBF greatly exceeds (perhaps 10–20 times over, in some brain regions) the oxygen needs of a local patch of active neurons [10,11]. This likely occurs because failure to deliver sufficient oxygenated blood will result in hypoxia and brain damage, thus potentially providing the type of evolutionary pressure resulting in the 'watering the entire garden for a single flower' phenomenon often used to describe the BOLD signal [10]. This overshoot phenomenon, however, creates an interpretational issue when considering the BOLD signal. If CBF, which relates, in part, to CBV based on changes in flow through capillaries/arterioles, consistently overshoots the needs of an active patch of brain, one must necessarily take into consideration how neurons and glia interact with the surrounding vasculature to produce such changes in blood flow [11,18,19].

2. The neurovascular unit: constraints on neurovascular coupling

The interaction between neural activity and the surrounding vasculature is often referred to through the concept of the neurovascular unit (NVU) [20]. Both 'feedback' and 'feed-forward' neural signals directly influence the BOLD signal. Feedback signals refer to changes in blood flow driven by dips in oxygen concentration/ATP/glucose, typically due to consumption by active neurons in a brain area. This vasodilation of arterioles may sometimes be distant from local active sources and can be considered a response to low concentrations of needed metabolites—whatever the cause. Feed-forward signalling, in contrast, refers to local changes in blood flow through capillaries driven more directly by increases in glutamate (due to synaptic signalling from incoming afferents). Such increases in glutamate trigger astrocytes and vasoactive agents that interact directly with local capillaries [11,21]. The overshoot phenomenon mentioned earlier, in which CBF greatly outpaces metabolic demand [10], is likely a consequence of such feed-forward signals driven by incoming synaptic activity from neighbouring brain areas [22]. Interestingly, there may even be situations in which the haemodynamic response can influence neural activity, for example, increases in pressure with penetrating arterioles can suppress or enhance pyramidal cell activity [23,24]. Together, these findings suggest that neural activity alone does not drive the BOLD signal: in fact, it is a complex, bidirectional interaction. Consistent with this idea, studies looking at both CBF and neural activity suggest that changes in CBF can occur with no corresponding changes in neural activity [25] and that glial activity in isolation can result in changes in CBF [9].

The idea that the BOLD signal is fundamentally intertwined with the actions and mechanisms of the NVU creates

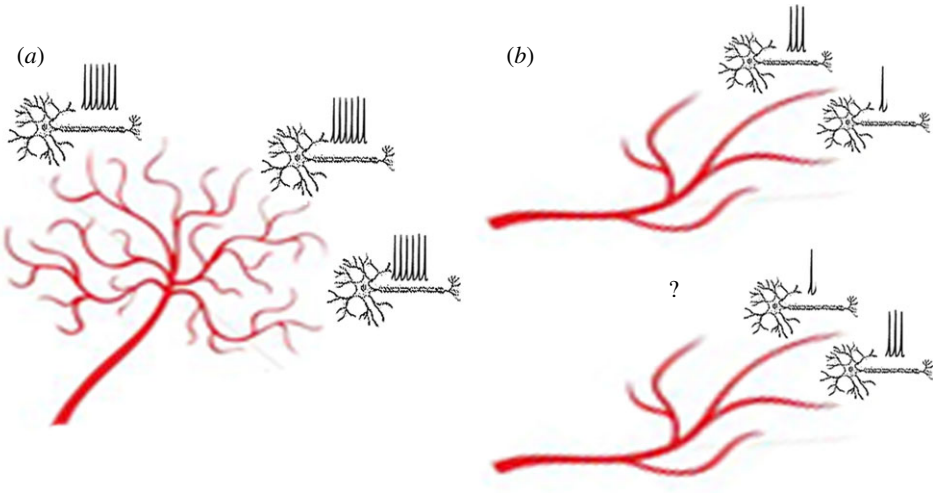

Figure 1. How the vasculature affects BOLD-neural correlations. Two examples of how the vasculature puts important constraints on how precisely one can relate neural activity to BOLD signal changes. (*a*) A dense capillary network as one might find in primary sensory cortices. A small ensemble of neurons (each shown as a single neuron) can trigger separate increases in blood flow, allowing discrimination of the activity of individual neurons. (*b*) A sparse capillary network, such as might be found in the hippocampus, places significant constraints on how precisely one can measure the activity of small ensembles of neurons. As shown here, it is not possible to distinguish different levels activity from two neighbouring ensembles that both trigger blood flow changes from the same capillaries/arterioles. (Online version in colour.)

somewhat of a paradigm shift in terms of how one might think about the BOLD signal [20]. Undoubtedly, there are situations where neural activity correlates strongly with changes in the BOLD signal, demonstrated clearly and consistently in numerous species in sensory cortices [26–31]—issues I will discuss in more depth shortly. These situations might be expected in areas like the visual cortex, in which the cortical layers recorded from (layers 1–6) have a clear columnar organization and relationship to underlying vasculature [32]. In situations in which the NVU differs from the sensory cortices, however, one might reasonably expect differences in neurovascular coupling in other brain areas. One important constraint with the BOLD signal is that it is sluggish (with about a 1–2 s delay to onset and about a 6–10 s response period overall). Therefore, situations in which proximate neural ensembles are simultaneously active, particularly in cases of sparse vascularization, would be difficult to disentangle with fMRI (figure 1). Similarly, because both inhibitory (e.g. GABAergic) and excitatory (e.g. glutamatergic) neural activity have metabolic demands [33], disentangling which particular mixture of the two is driving the BOLD signal will also be difficult.

This issue also relates to the degree of sparsity versus distributed neural coding schemes within a region, in other words, how many groups of neurons are active and in what manner [34]. If sparse neural signals are present, this may result in relatively small changes in BOLD compared with other brain regions that employ a more distributed response (e.g. figure 1). The density of the vasculature itself is particularly relevant: if capillary/arteriole spacing is dense and well connected with astrocytes communicating with active neurons, detecting even small changes in neural activity will be possible (figure 1*a*). By contrast, for sparse vasculature in which blood flow is less precisely modulated by local neural activity, such neurovascular coupling may be less predictable and corresponding neural codes more difficult to decipher (figure 1*b*). I will consider these issues in more depth shortly when I compare neurovascular coupling in the hippocampus with that in sensory cortices. Sparse versus distributed coding is also important to what types of analyses are useful for interpreting BOLD signal changes. For example, as I will explore in more depth shortly, multivariate pattern analysis (MVPA), rather than univariate modelling, is likely better suited to capturing such underlying changes in distributed coding of populations of neurons. This is because MVPA is sensitive to changes in both strongly and weakly active voxels, although one trade-off with this increased sensitivity to population responses is MVPA cannot inform about how a single voxel might relate to a small group of neurons within a voxel.

3. What does one mean by neural activity?

Before discussion of studies that have looked at how the BOLD signal relates to underlying neural activity, it is worth defining exactly what one means by 'neural activity.' Interestingly, this definition of 'neural activity' is probably most accurately referred to as 'what one can observe with existing extracellular and/or calcium imaging techniques' rather than an absolute measure of something more specific like the number of action potentials emitted by a single neuron in isolation or glutamatergic synaptic activity specifically. This is because extracellular recordings involve the need both to identify *post hoc* individual neurons (which can be imprecise and inaccurate [35]) and to apply specific filter setting to observe the local field potential (LFP) [36]. In addition, the signal produced from extracellular recordings is heterogeneous in origin and exactly what types of underlying neural signals they represent remains unclear. For example, there is no clear idea when something like synaptic activity (which is thought to dominate the lower frequency bands) ends and action potentials (which are thought to dominate the higher frequency bands) begin [36], which will become relevant in my subsequent discussions.

One important component of the LFP derives from a low-pass filter of extracellular recordings [37]. This signal typically contains semi-periodic fluctuations ranging from very low frequency (less than 1 Hz, infraslow), to low frequency

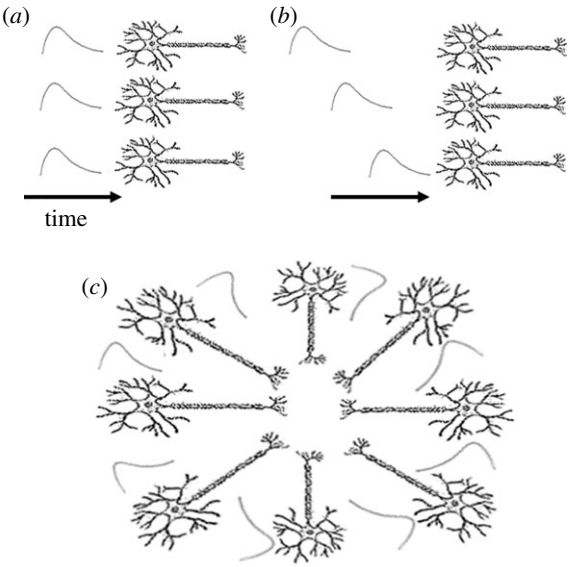

Figure 2. Multiple and ambiguous origins of the local field potential. Spatio-temporal organization plays a critical role in what synaptic potentials will contribute to the low-pass local field potential. (*a*) Fibres arranged parallel to each other with synaptic potentials occurring close in time will produce sinks and sources that will allow maximum linear summation. (*b*) By contrast, temporally asynchronous synaptic potentials will produce significantly fewer summations as sources will dissipate rapidly, resulting in less summation. (*c*) Fibres arranged in a perpendicular or closed-loop structure (such as the hippocampus) would be expected to produce little net contribution to the local field potential, particularly when measured outside of the structure. When measured inside of the structure, it will be difficult to discriminate cancelling, interfering and summating sources to the local field potential.

(1–20 Hz, delta, theta, alpha, beta), to low/mid-range gamma (20–60 Hz), to high-gamma (greater than 60 Hz) [38–42]. Signals in the LFP below 60 Hz are likely the result primarily of summations of excitatory synaptic potentials [37], which refers to infraslow, delta, theta, alpha, beta and low–mid-range gamma bands. Note that the 'cutoff' for the low-pass LFP varies by studies, with some using thresholds as low as 30 Hz (e.g. [28]). Other electrophysiological signals also undoubtedly contribute to the 'low-pass' LFP, however, including inhibitory synaptic potentials, subthreshold potentials due to other neuromodulators, and backpropagating signals [37]. For simplicity's sake, I focus primarily on excitatory post-synaptic potentials and their putative contributions to the LFP as these are typically thought to dominate in most recording situations [43]. I shall consider the high-pass signal of the LFP (greater than 60 Hz), referred to alternatively as 'broad-band gamma' and 'high-gamma', shortly, although note again that this threshold can vary by studies, with some studies using values as high as 80 Hz (e.g. [44]).

A critical component dictating how these synaptic potentials summate in the low-pass LFP is how neural fibres are arranged relative to each other [43]. This idea can be readily illustrated by considering a simplistic situation of either parallel or perpendicularly arranged fibres in a brain structure (figure 2). For example, synaptic potentials from two parallel fibres that co-occur in time will summate, resulting in the active flow of charge from one region to another (figure 2*a*, *b*). This separation of charge due to current flow is referred to as a dipole or a sink/source, depending on the flow of charge. By contrast, synaptic potentials from fibres arranged perpendicularly or with flows in opposing directions will produce significantly lower or no net dipole at all when measured with a distal electrode (figure 2*c*). Electrodes placed within such closed-loop structures will record a combination of summating and interfering signals. In this way, both the arrangement of fibres and temporal synchrony are critical determinants of what types of signals will manifest in the LFP.

The other critical component that can readily be extracted from extracellular recordings is the higher frequency signal, often referred to as high-pass gamma-band activity or 'high-gamma'. This signal contains a significant portion of spikes from nearby neurons firing in a synchronous manner [42,45]. The main difference between the high-pass and low-pass LFP is that the high-pass signal contains faster action potentials while the low-pass signal contains comparatively slower summating synaptic potentials [37]. In both cases, though, the arrangement of fibres and their temporal synchrony are critical determinants of what neurons will contribute to either component of the LFP [37]. Again, it is also important to note that neither the low- nor high-pass signal can be considered 'pure' and the high-pass signal, in particular, contains contributions from synaptic activity as well [37,42,45]. When filtering above approximately 300 Hz (with this cutoff itself somewhat variable, either lower or higher depending on the study), one can also obtain multi-unit activity (MUA), and with additional analysis, action potentials from individual neurons [35], often referred to as single-unit activity or SUA.

The variable genesis of electrophysiological recordings suggests that the basis for these signals themselves might be regionally variable [5]. In a location like the visual cortex, which has a columnar structure [46], or motor cortex, which has an organized mapping based on the representation of body parts [47], one might expect that local interactions and gamma-band modulations from the thalamus will exert a powerful effect on the LFP [45]. In this instance, one might expect the LFP to be dominated by changes in high- and low-gamma-band activity during visual or motor stimulation, consistent overall with such electrophysiological observations [31,48–50]. Similarly, one might expect that anatomically neighbouring orientation-selective neurons would be active during stimulation by a bar of light, resulting in synchronous discharge and emergence of modulations in the high-gamma band due to temporally synchronous MUA [51]. This might, in turn, bear some connection to why relatively strong neurovascular coupling is typically observed in the visual cortex, often between multi-unit firing, mid/high-gamma-band activity and the BOLD signal [32].

By contrast, for an area like the hippocampus, one might expect somewhat of a different relationship [5]. The septal nucleus provides a strong drive within the theta band (4–8 Hz) and thus the LFP is typically more dominated by changes in theta-band activity than gamma [52]. Similarly, given observations of sparse and anatomically uncorrelated place cells [34,53], activity in hippocampal pyramidal neurons would be unlikely to have much influence on higher frequency activity, although some of this might depend on the electrode recordings and their location within the hippocampus. The hippocampus itself is often referred to as a 'closed-loop' structure because, anatomically, the different subfields form an interconnected and (in the coronal plane) nearly ovular structure [54,55]. As such, one might expect a clearly decipherable summation of local activity within the hippocampus to be difficult to observe (figure 2*c*). Consistent with such observations, neurovascular coupling in the hippocampus, if

present, often appears within the theta band and less commonly with underlying neural activity [56]. I will explore these two structures in more detail when I consider neurovascular coupling in the neocortex and hippocampus shortly.

4. Neurovascular coupling in the visual and somatosensory cortex: does this provide us with a Rosetta Stone?

The Rosetta Stone, when discovered, allowed definitive translation of Egyptian hieroglyphics, which were unknown at the time. This was possible because alongside hieroglyphics was ancient Greek text that was inscribed for the same proclamation. Similarly, one of the central goals of research in neurovascular coupling is to determine what electrophysiological signals underlie the BOLD signal. The idea of a Rosetta Stone in the context of fMRI is that one could readily interpret increases and decreases in the BOLD signal provided one knew exactly how this related to underlying changes in neural signalling. The issues I will discuss, however, with attempting a Rosetta Stone for fMRI are that: (i) regional variability makes a single Rosetta Stone untenable, (ii) the contributions to BOLD and electrophysiology are heterogeneous, involving different scales which themselves may have varying and difficult to pin down contributions, (iii) sparse neural coding schemes, in particular, may be difficult to observe with fMRI, and (iv) signal quality may vary with fMRI independently of electrophysiology, confounding direct comparisons.

To determine how electrophysiological signals relate to the BOLD signal, one requires some means of comparing the two signals, either simultaneously or serially. Studies in non-human animals have involved both simultaneous and serial comparisons of signals such as BOLD, CBV, CBF and $CMRO_2$ with different components of electrophysiological recordings. Studies in humans involving invasive recordings (allowing access to deeper brain structures) typically use serial comparisons because of dangers with electrode heating and other safety concerns with implanted electrodes in a strong magnet [57]. Here, I will focus first on studies in non-human animals and then attempt to tie this in with humans. It is important to note that when correlating electrophysiological and haemodynamic signals, they involve inherently different temporal resolutions, which must be taken into account. Specifically, electrophysiological signals can occur on the time scale of milliseconds (particularly action potentials, which last about 1–3 ms) while the BOLD signal occurs on the scale of seconds (6–20 s, depending on the experimental design). To compare the two, one must convolve faster electrophysiological signals with some function representing the haemodynamic response and account for its delay. Another option is to compare electrophysiology and the haemodynamic response function (HRF) separately with ongoing behaviour, although this still requires some modelling of the BOLD response based on behavioural stimulation. Importantly, there are a number of different functions one can use to convolve to model the haemodynamic response, with a common choice being a double gamma function, although even the haemodynamic response function can vary by brain region [58].

In seminal studies conducted in the visual cortex by Nikos Logothetis's laboratory in both anaesthetized and awake behaving monkeys [26,59,60], the authors recorded BOLD, LFP and MUA simultaneously in the visual cortex. The authors found that increases in BOLD fMRI strongly correlated with increases in the low-pass LFP recorded simultaneously at nearby electrodes ($r^2 = 0.52$). Putative MUA activity, which involved a high-pass signal, showed a significant although weaker correlation ($r^2 = 0.45$) with BOLD than the low-pass LFP [26]. Subsequent studies also suggested that both increases and decreases in BOLD in the monkey visual cortex could be related to increase and decreases in the low-pass LFP [59]. Similar findings have also been reported in rodent somatosensory cortex [61,62]. These findings, which have been extensively reviewed elsewhere [32], suggested that synaptic activity, as reflected in the low-pass LFP, and, to a lesser extent, MUA, underpinned much of the BOLD signal.

Findings suggesting a three-way correlation between BOLD, the gamma-band LFP and MUA have also been reported from sensory areas in humans such as the primary auditory cortex [27,28]. In one study by Mukamel *et al*. [28], the authors employed microelectrode recordings (approx. 40 µm platinum–iridium electrodes) in a group of patients watching a movie and compared them with a separate group of healthy participants watching the same movie. Mukamel *et al*. [28] averaged the spike rate of about 50 neurons recorded from two patients to generate predicted BOLD responses in the auditory cortex in healthy participants. When comparing with the filtered LFP above 40 Hz, both BOLD and spike rate (MUA) correlated strongly, with correlations (r^2) between BOLD and spike rate comparable to Logothetis *et al*. [26] ($r^2 \approx 0.4$–0.5). These findings suggested that a significant per cent of the variance in the BOLD signal could potentially be related directly to changes in action potentials and synaptic activity [28]. Based on both the Logothetis *et al*. [26] and Mukamel *et al*. [28] studies, one version of a Rosetta Stone, which I term the BM Rosetta Stone (BOLD–LFP–MUA), is that the BOLD signal correlates with both low-pass and high-pass gamma-band activity. Because synaptic and spiking activity are correlated in sensory areas in some studies, the BOLD signal should reflect both low-pass gamma-band activity and MUA [63].

One problem with this idea, however, is that the synaptic and MUA components of broad-band gamma activity appear dissociable. Ray & Maunsell [37] studied this issue in the primate visual cortex by varying the size of a stimulus presented [37]. This allowed them to dissociate the low-pass gamma-band LFP from high-pass gamma. Varying the size of the stimulus presented to the monkey resulted in changes in low-pass gamma but not high-gamma. In another study, Ray *et al*. [42] averaged individual neuron spiking activity to compare with high-gamma and activity. While increases in the firing of neurons explained some of the increases in high-pass gamma activity, synchrony among neurons provided a significantly stronger prediction of high-gamma activity [45], consistent with earlier arguments about the importance of spatial and temporal organization of cells that contribute to the LFP. Together, these findings suggest that a significant component of high-pass gamma activity involves contributions from spiking activity, which in turn relates primarily to the degree of synchrony among these neurons and is separable from low-pass gamma-band activity.

Consistent with these ideas, when explicitly dissociated, low-pass gamma-band activity correlates more strongly with the BOLD signal than MUA [31,64,65]. Studies in the primate

visual cortex demonstrated that the abolition of spiking, through either manipulation of pharmacology [64] or stimulus characteristics [65], resulted in robust BOLD/$CMRO_2$ and LFP correlations. Thus, even in the absence of spike rate, which could be accomplished either pharmacologically or behaviourally, the low-pass gamma-band LFP appeared to be the clearer correlate of BOLD signal changes. It is also important to note that even in the original Logothetis *et al*. [26] study, the correlation was lower between spike rate and BOLD than the low-pass LFP and BOLD, with subsequent studies in awake behaving primates also suggesting the low-pass LFP was a significantly stronger correlate. Finally, it is important to note that comparisons between BOLD and electrophysiology require temporal smoothing. Thus, particularly given its transient and temporally varying nature, single-neuron activity, when compared with BOLD, may be particularly sensitive to the smoothing kernels applied.

Therefore, instead of concluding that BOLD can reflect both multi-unit spiking activity and synaptic contributions from the LFP, a second version of the Rosetta Stone suggests that BOLD primarily reflects low-pass gamma activity. Because low-pass LFP activity should be primarily synaptic and not action potentials, the BSA (BOLD–synaptic activity) Rosetta Stone suggests that the BOLD signal largely reflects synaptic activity [22]. This has led to the idea BOLD reflects the input to a brain region (synaptic activity) while MUA reflects the output [66]. As I will discuss, these two 'BOLD Rosetta Stones' hinge on several critical assumptions, which will be carefully evaluated in the next sections.

5. Problems with the BM/BSA Rosetta Stone: interpreting correlations

The BM version of the Rosetta Stone rests on the idea that the BOLD signal shows a positive correlation with gamma-band activity in sensory cortices (e.g. corr(BOLD,gamma) > 0) and that broad-band gamma activity, in many situations, shows a positive correlation with MUA (e.g. corr(gamma, MUA) > 0) [63]. Some have interpreted this to indicate that the three should, therefore, be interrelated, allowing direct linkage between findings from the three measures (e.g. [67]). Simply because the correlation between gamma and BOLD is greater than zero, and that between gamma and MUA is greater than zero, does not necessarily mean, however, that the correlation between BOLD and MUA is, therefore, consistently greater than zero. For example, rain may often be correlated with the use of galoshes. Galoshes may sometimes be correlated with age, in other words, older adults are more likely to wear galoshes. This does not mean, however, that rain is correlated with the presence of older adults. Or put another way, correlations are not transitive, and corr(A,B) > 0, corr(B,C) > 0 does not necessarily mean that corr(A,C) > 0.

More generally, while BOLD, gamma-band power and MUA may covary in some cases this does not imply that the same factors affecting one, as in the example given, affect the other. For example, in the Logothetis *et al*. [26] study, even though BOLD changes correlated with gamma-band power changes, and BOLD changes also correlated (to a lesser extent) with changes in MUA, at least some of this variance related to the similar time courses of MUA and the LFP [22]. Note that this is an inevitable consequence of the fairly fast activation that one sees in both the low-pass LFP and MUA to behavioural stimulation [68]. Indeed, as pointed out above, when MUA is explicitly manipulated or blocked, BOLD and the gamma-band LFP continue to correlate significantly. This suggests that synaptic activity influences BOLD instead of MUA directly influencing BOLD.

What about the BSA Rosetta Stone, which argues that changes in synaptic activity, as measured by the low-pass gamma-band signal, underlie BOLD signal changes? The problem here is that regional variability in any of these three measures makes it unlikely that this relationship will hold for other brain areas or even different substructures of the same brain area. Li *et al*. [69] addressed this issue by investigating evoked activity in the glomerular (GL), mitral cell (MCL) and granular cell layers (GCL) of the olfactory bulb [69]. Rats received odours while undergoing BOLD and LFP recordings in separate sessions. BOLD signal changes in response to different odours were strongest in GL, then MCL, with the weakest activation in GCL (GL > MCL > GCL). By contrast, low-gamma-band activity was strongest in GCL compared with all other layers such that GCL > GL > MCL, with the other frequencies (beta and high-gamma) showing a less consistent relationship with BOLD. Finally, the BOLD–LFP relationship varied by temporal epoch, with variation in responses for the different LFP bands during the odour onset, sampling period, odour off and recovery period. Together, these results suggest that the BOLD–LFP relationship varied by layer within the olfactory bulb and task component, which the authors argued likely related to neural arrangement and vascular factors that differ across layers of the olfactory bulb.

In a similar vein, Herman *et al*. [70] found additional variability between the BOLD signal, the LFP and MUA across cortical layers in the somatosensory cortex when including separate measurements of $CMRO_2$, CBF and CBV. Specifically, the magnitude of the BOLD signal, MUA and gamma-band LFP often varied in opposite directions across upper, middle and lower layers of the sensory cortex. Interestingly, MUA correlated across layers with $CMRO_2$ measurements, which might be expected based on our earlier arguments about a close relationship between spiking activity and fast utilization of oxygen. The low-pass gamma-band LFP and CBF measures also correlated, although less consistently, suggesting that the LFP may be better related to a separate component of the BOLD signal, regional changes in blood flow. These findings suggest that different components of the BOLD signal might dissociate depending on regional vasculature and local metabolic demands. It is important to note that both of these studies involved primary/secondary sensory areas and, although low-pass gamma correlated with BOLD in many instances, there was both regional and task-related variability across different layers of cortex that mediated this relationship.

6. Regional variability in BOLD–LFP coupling across the brain

The studies discussed above so far suggest that BOLD neural coupling may vary as a function of layer and component of the BOLD signal (i.e. CBF versus $CMRO_2$). The studies above, however, all focused on a single sensory brain region in non-human animals. By contrast to animal recordings, most invasive and non-invasive comparisons with fMRI in humans typically involve broader coverage across the brain, including associative and non-neocortical areas (i.e.

three-layered versus six-layered). It is, therefore, useful to consider how the BOLD–LFP relationship might vary when comparing between different brain regions.

In a study by Conner *et al*. [71], patients performed a naming task in the scanner and then again after undergoing ECoG implantation. The authors focused on LFP recordings from ECoG grid recordings and did not record MUA, although other studies have related MUA activity, in some cases, to high-pass gamma-band activity recorded with ECoG [41,42]. Conner *et al*. [71] found that low-pass gamma and beta accounted for about 22% of the variance in the BOLD signal across the recording location. The brain region, however, contributed significantly greater variability to this relationship (28%). To illustrate some of the regional variability that Conner *et al*. [71] observed, *theta-band* activity was the strongest correlate of BOLD in superior temporal gyrus. By contrast, low–mid-gamma-band activity was the strongest correlate in the postcentral gyrus. These findings suggest that regional variability, for example, differences in local vasculature and arrangements of neural fields contributing to the LFP, also contributes significantly to neurovascular coupling.

Kujala *et al*. [72] performed a similar comparison using MEG and fMRI in healthy participants. Participants performed silent reading, and analyses employed a partial least-squares method to identify different factors contributing to BOLD across frequency bands. Kujala *et al*. [72] again found significant regional variability. Many brain regions showed a correlation between BOLD and low-pass gamma-band activity (as high as $r^2 \approx 0.36$ in some cases), with the exception of the precentral gyrus, which showed the opposite pattern (negative correlations for high-pass gamma, e.g. as high as $r^2 \approx 0.18$). There was also variability within the gamma band, with some regions showing stronger correlations with high-pass gamma-band activity and others showing stronger correlations with low-pass gamma-band activity. For example, middle frontal gyrus versus lingual gyrus showed opposite relationships with BOLD and components of gamma. Similarly, within the lower frequency bands, some regions showed opposite correlations such as theta with BOLD in middle temporal gyrus versus and beta with BOLD in superior frontal gyrus. Together, these findings suggested no consistent relationship across different frequencies bands, and while gamma-band activity broadly showed the most consistent positive relationship with BOLD, not all regions displayed this pattern and there was significant variability within the gamma band itself.

7. Why does regional variability arise? The impact of regional vascular differences

Using microelectrode recordings in the human medial temporal lobe and comparing with high-resolution fMRI (approx. $1.5 \times 1.5 \times 3$ mm voxels) in patients, Ekstrom *et al*. reported a correlation between BOLD and the theta-band LFP ($r^2 = 0.16$) and no correlation between BOLD and MUA [56]. Even this relationship, however, varied by brain region as we found that only positive changes in the BOLD signal correlated with theta-band changes within the hippocampus. Finally, we found no significant correlation between any LFP band and MUA/single neurons across the medial temporal lobe. Together, these findings suggested that: (i) the BOLD–gamma-band correlation does not hold in the hippocampus, a structure in which theta-band activity is most often observed as the dominant signal within the LFP, and (ii) the hippocampus may show additional variability in the BOLD signal compared with other brain regions within the medial temporal lobe (see also [73,74]). We suggested several possible reasons for these findings: variations in neurovascular coupling, which might be particularly pronounced in the hippocampus owing to sparse capillarization, sparse neural coding schemes in which few neurons are active, and domination of the LFP by theta-band activity due in part to cholinergic modulation from the septum [5]. Here, I explore these explanations in light of new supportive findings and also consider a fourth factor: variations in fMRI signal strength.

As discussed at the beginning of this paper, neurovascular coupling is more complex than the idea that greater neural activity results in feedback signals that trigger greater vascular constriction [20]. While neural activity can influence blood flow/volume through feedback, incoming neural activity can also influence CBF/CBV. Changes in CBF/CBV can also occur in an anticipatory fashion [25] and the vasculature itself can, in some instances, influence neural activity [23,24]. The effect of vascular differences on BOLD would be expected to be particularly pronounced in cases in which the capillarization of a brain area is sparse like the hippocampus [75]. As an example of when this can be an issue in the hippocampus, Shaw *et al*. [76] compared activation in the CA1 region of the hippocampus with the visual cortex in mice undergoing optogenetic stimulation of glutamatergic neurons. They coupled this stimulation with optical imaging of CBF, CBV and $CMRO_2$. Consistent with sparse capillarization within the hippocampus, resting blood flow and oxygenation were lower in the hippocampus compared with the visual cortex. In addition, the same degree of stimulation in CA1 as the visual cortex led to less blood vessel dilation, which in turn related to how responsive the vasculature was to stimulation in the hippocampus versus neocortex. Neural synchrony and enzymatic responses of astrocytes, however, did not differ between brain regions. These findings suggest that the vasculature itself puts constraints on how neural activity drives CBF, $CMRO_2$ and CBV. Further consistent with these findings, calibrated fMRI studies suggest lower coupling levels in the hippocampus and other deep brain structures compared with neocortical areas [15,77].

8. Sparse versus distributing neural coding schemes

Place cells, neurons that respond at specific locations as a rat navigates, represent a nice example of how neurons in the hippocampus might code an abstract variable like location in the environment [78,79]. Somewhat unlike orientation cells in the primary visual cortex, however, place cells show sparse coding, meaning that few place cells fire at any given moment as a rat explores an environment. For example, computational estimates, based on recordings of multiple place cells during exploration, suggest that a small fraction of such cells are active at any given time as a rat explores an environment [34]. At the same time, place cell responses in the hippocampus do not show a structured anatomical organization. In other words, two place cells that fire nearby each other on a maze have the same chance of being located next to each other anatomically within the hippocampus as two

place cells that fire at distant locations [80]. The combination of both sparse coding and a lack of clear anatomical organization of functional responses has important implications for the BOLD signal. This is because when few cells fire that are not anatomically proximate, their collective activity is unlikely to be sufficient to trigger a change in BOLD in a $1 \times 1 \times 1$ mm voxel.

Consider, for example, exploration of a specific location in space. Based on the discussion above, a small number of place cells should be active at any given location and the cells themselves should be distributed fairly uniformly across subfields of the hippocampus. Given that the capillarization of the hippocampus is also sparse, this suggests that location responses will evoke little if any increase in BOLD signal voxels (e.g. figure 1*b*). In fact, one might expect that such signals would be both too weak at a single voxel and too anatomically disparate to evoke much of a BOLD signal change at all. Consistent with this, recent attempts to find evidence for place coding within the hippocampus using fMRI strongly suggest null findings, with overall no support for location coding using BOLD [81]. This contrasts with the visual cortex, where studies have observed orientation-selective responses using fMRI and MVPA [82,83], suggesting different functional and anatomical organization.

9. fMRI signal quality

The last issue to consider is varying signal quality obtained with fMRI. This was highlighted in a recent study by Tsao *et al.* [84] based on identified areas of activation to faces (which they termed 'face patches') using fMRI. In their study, Tsao and coworkers [84] compared how well such functional 'patches' code facial identity using both BOLD and single neuron recordings in non-human primates. They employed MVPA of both single neuron and fMRI to attempt to understand how patterns of activity might relate to different behavioural variables in their study. Classification of different faces based on single-neuron firing patterns improved dramatically as the authors moved posteriorly to anteriorly within such patches. fMRI classification, however, showed somewhat of the opposite pattern, resulting in little correlation between fMRI voxel patterns of faces and single neurons at the same locations. The authors performed analyses of signal-to-noise within the patches recorded from the monkeys and found that anterior sections, which were closer to the sinuses and ventricles, typically had lower signal-to-noise than those posterior. Thus, the lower signal quality seemed to play an important role in what sort of information could be decoded from the BOLD signal. This issue is also relevant for areas like the anterior hippocampus and entorhinal cortex, which also suffer from signal dropout and distortion, where recent attempts have tried to tie BOLD responses to those of grid cells [85].

10. The road forward: if not a Rosetta Stone, then what?

As I have highlighted above, neurovascular coupling shows a fairly consistent relationship in areas like sensory cortices, where gamma-band activity, and, to a lesser extent, MUA, correlate with BOLD. This has led to the hope that perhaps a Rosetta Stone can be applied across the brain such that one could tentatively assign BOLD signal changes to gamma-band changes [63,86]. As discussed, though, the major issue with this approach is that neurovascular coupling, much like the BOLD signal itself [58,87], is regionally variable. In other words, while the BOLD signal may correlate with the low-pass gamma-band signal in some cases, it correlates with high-gamma-band activity in others, with theta-band activity in others, and with no component of the LFP consistently in others. As discussed, this is likely due to the fact the BOLD signal itself is a multifaceted signal comprising CBF, CBV and $CMRO_2$. These contributions themselves show regional variability, as does their integration within the NVU. In addition, neural coding schemes, for example, sparse versus distributed coding, and the organization of neurons within a structure, are important determinants of how action potentials and synaptic changes will contribute to the LFP and MUA. As all of these factors can vary by region, and even cortical layer, thus they make a single Rosetta Stone unlikely.

The above arguments lead to the possibility, however, that one could approach the problem of deciphering what the BOLD signal means as far as underlying neural activity by considering other factors, like neural synchrony [88] or nonlinear transfer functions [89]. This could potentially lead to a situation in which we have functions for every brain region we might be interested in telling us when and how BOLD will relate to synaptic versus spiking activity. While such a nuanced Rosetta Stone would certainly be useful, it should also take into consideration task variability [25], which might quickly make such a look-up table impractical.

Another approach instead, given some of the variability in spatial relationship between BOLD and neural activity, might be to consider how distributed neural patterns code information, such as the example considered earlier regarding face 'patches' with fMRI. Such an approach is already implemented in some form by fMRI analyses that employ methods to look at patterns of voxels rather than specific clusters of voxels that are above or below some statistical threshold [90,91]. This approach, often referred to broadly as MVPA, looks at how changes in patterns of voxels relate to behavioural variables. Such methods fall into two broad categories, *pattern classification*, which typically involves machine learning algorithms, and *pattern analysis*, which typically involves correlating patterns of activity across thousands of different active units (e.g. voxels, single neurons or electrodes recording the LFP).

Pattern classification typically involves training a machine learning algorithm on a subset of trials involving neural activity and specific behavioural conditions and then subsequently testing whether the algorithm can correctly 'guess' the behavioural condition from 'test' neural data. Such methods have a rich history in fMRI [83,90,92–94]. Importantly, such methods often (but not always) apply no assumptions about the HRF at all and use normalized voxel intensities as neural input data to train the classifier. By contrast, *pattern analysis* techniques involve correlating the patterns of voxels (or single-neuron activity [95,96]) across active voxels to determine the extent to which patterns are the same or differ for behavioural conditions of interest (for example, successful versus unsuccessful retrieval [97]). Typically, pattern analysis employs some assumptions about the underlying HRF, although this too can vary by the methods applied. For example, finite impulse response (FIR) modelling techniques, often applied to pattern analysis with

fMRI [98], make minimal assumptions about the shape of the HRF [87,99], while other approaches employ canonical HRFs and then correlate the degree of such 'fits' across voxels. Importantly, the main advantage of both pattern classification and analysis (referred to as MVPA here) is that they pick up on both weakly and strongly active voxels, which can move in either direction relative to baseline.

By contrast, univariate approaches focus on modelling changes in the HRF one voxel at a time, typically as the same function across the brain, and then determine how well the convolution of this function with the behavioural variables of interest fit the observed fMRI patterns across all voxels in the brain. Subsequent analyses then focus on finding clusters of activation that exceed some threshold, allowing determination of whether activation in these clusters increased or decreased relative to baseline. The issue with this approach, however, is that an increase or decrease in activation is difficult to interpret directly in terms of underlying electrophysiological activity because the electrophysiological basis of the BOLD signal is regionally variable. In addition, the basis of LFP changes can include different contributions from action potentials, excitatory and inhibitory post-synaptic potentials—all of which are difficult if not impossible to determine for any given patch of tissue. Finally, the haemodynamic response function may be regionally variable [58,87], leading to ambiguity in terms of whether an increase or decrease in BOLD reflects possible true or false positives [100].

MVPA involving pattern classification, as discussed above, does not need to involve explicit modelling of the haemodynamic response function while pattern classification can involve some assumptions about the shape of the HRF depending on the approach. Importantly, though, because MVPA focuses on the population of activity rather than a single voxel of activity, the haemodynamic response function does not matter as much in this case because the distributed voxel patterns themselves are what drives information retrieval and not whether the signal correlates better with a hypothesized response function. This is advantageous in other ways because the BOLD signal can have its origins at arterioles (distal) or capillaries (local), particularly at conventional field strengths [21,101], which MVPA naturally captures by considering a spread of voxels. The third advantage of MVPA with regard to better capturing underlying electrophysiological activity relates specifically to the fact that MVPA considers the distributed patterns of strongly and weakly active voxels and how voxels relate to a behavioural variable rather than considering whether activation goes up or down sufficiently at a subset of restricted voxels. For example, LFP responses may also reflect a distributed signal, particularly for lower frequency bands [102], and therefore methods that capture this spatial spread are better suited to capturing information carried by underlying electrophysiological signals. Also, the LFP, and BOLD signal by proxy, could involve excitatory or inhibitory signals that are almost impossible pinpoint and, therefore, it is more meaningful to consider the patterns of activity rather than whether they go up and down.

By focusing on patterns and their relationship to information, rather than focal activation going up or down in response to a stimulus, one can avoid problematic interpretations inherent in interpreting BOLD related to baseline, and, perhaps most importantly for our current considerations, the magnitude of those changes. Such MVPA techniques can also readily be performed on numerous different types of electrophysiological recordings and related to perceptual and memory processes, including scalp EEG, MEG, ECoG and single-neuron activity [84,95,96,103,104]. Some studies in fact suggest striking consistencies between MVPA of fMRI and single-neuron recordings in monkeys [105,106]. Since the scale of the patterns of voxels is somewhat arbitrary, one can increase or decrease the resolution of neural recordings to more directly compare with MVPA techniques from fMRI by filtering or averaging. MVPA also does not typically employ spatial smoothing, allowing determination of how information in each voxel might relate to electrophysiological signals independently from their neighbour. In this way, one can perform more principled comparisons of what sorts of information are carried at the different scales of fMRI and neural recordings, although one loses the ability to directly relate an increase or decrease at a specific voxel to a corresponding change in neural activity within that voxel.

11. Conclusion

The considerations presented here suggest that regional factors play a significant role in neurovascular coupling. Such considerations, based on differences in vascular neural regional organization, put significant constraints on the likelihood that a single Rosetta Stone will work for the entire brain. It is important to note, however, that nuanced and informed interpretations of fMRI are still very much possible, particularly if one employs multivariate methods that consider patterns of voxels and their relationship to information coding rather than focal activation. Using such methods, one can gain insight into what sorts of information a brain region codes at the level of fMRI and relate this to what sorts of information the LFP and MUA code. Given that these signals also exist at different spatial scales (with single neurons being the smallest for extracellular electrophysiology), it may be that one can learn different sorts of information by focusing on these different scales. Thus, rather than employing a Rosetta Stone to interpret fMRI, one may instead think about what sorts of complementary and convergent information one can obtain from the different spatio-temporal scales provided by fMRI and electrophysiology.

Data accessibility. This article has no additional data.

Competing interests. I declare I have no competing interests.

Funding. A.D.E. was supported by NIH/NINDS: R01NS076856.

References

1. Hyde JS, Biswal BB, Jesmanowicz A. 2001 High-resolution fMRI using multislice partial *k*-space GR-EPI with cubic voxels. *Magn. Reson. Med.* **46**, 114–125. (doi:10.1002/mrm.1166)
2. Penny WD, Friston KJ, Ashburner JT, Kiebel SJ, Nichols TE 2011. Statistical parametric mapping: the

analysis of functional brain images. London, UK: Elsevier.

3. Jenkinson M, Bannister P, Brady M, Smith S. 2002 Improved optimization for the robust and accurate linear registration and motion correction of brain images. *Neuroimage* **17**, 825–841. (doi:10.1006/nimg.2002.1132)
4. Cox RW. 1996 AFNI: software for analysis and visualization of functional magnetic resonance neuroimages. *Comput. Biomed. Res.* **29**, 162–173. (doi:10.1006/cbmr.1996.0014)
5. Ekstrom AD. 2010 How and when the fMRI BOLD signal relates to underlying neural activity: the danger in dissociation. *Brain Res. Rev.* **62**, 233–244. (doi:10.1016/j.brainresrev.2009.12.004)
6. Ogawa S, Tank DW, Menon R, Ellermann JM, Kim SG, Merkle H, Ugurbil K. 1992 Intrinsic signal changes accompanying sensory stimulation: functional brain mapping with magnetic resonance imaging. *Proc. Natl Acad. Sci. USA* **89**, 5951–5955. (doi:10.1073/pnas.89.13.5951)
7. Hyder F. 2004 Neuroimaging with calibrated fMRI. *Stroke* **35**, 2635–2641. (doi:10.1161/01.STR.0000143324.31408.db)
8. Ogawa S, Lee TM. 1990 Magnetic resonance imaging of blood vessels at high fields: *in vivo* and *in vitro* measurements and image simulation. *Magn. Reson. Med.* **16**, 9–18. (doi:10.1002/mrm.1910160103)
9. Takata N *et al.* 2018 Optogenetic astrocyte activation evokes BOLD fMRI response with oxygen consumption without neuronal activity modulation. *Glia* **66**, 2013–2023. (doi:10.1002/glia.23454)
10. Fox PT, Raichle ME. 1986 Focal physiological uncoupling of cerebral blood flow and oxidative metabolism during somatosensory stimulation in human subjects. *Proc. Natl Acad. Sci. USA* **83**, 1140–1144. (doi:10.1073/pnas.83.4.1140)
11. Raichle ME, Mintun MA. 2006 Brain work and brain imaging. *Annu. Rev. Neurosci.* **29**, 449–476. (doi:10.1146/annurev.neuro.29.051605.112819)
12. Malonek D, Grinvald A. 1996 Interactions between electrical activity and cortical microcirculation revealed by imaging spectroscopy: implications for functional brain mapping. *Science* **272**, 551–554. (doi:10.1126/science.272.5261.551)
13. Hu X, Yacoub E. 2012 The story of the initial dip in fMRI. *Neuroimage* **62**, 1103–1108. (doi:10.1016/j.neuroimage.2012.03.005)
14. Davis TL, Kwong KK, Weisskoff RM, Rosen BR. 1998 Calibrated functional MRI: mapping the dynamics of oxidative metabolism. *Proc. Natl Acad. Sci. USA* **95**, 1834–1839. (doi:10.1073/pnas.95.4.1834)
15. Restom K, Perthen JE, Liu TT. 2008 Calibrated fMRI in the medial temporal lobe during a memory-encoding task. *Neuroimage* **40**, 1495–1502. (doi:10.1016/j.neuroimage.2008.01.038)
16. Smith AJ, Blumenfeld H, Behar KL, Rothman DL, Shulman RG, Hyder F. 2002 Cerebral energetics and spiking frequency: the neurophysiological basis of fMRI. *Proc. Natl Acad. Sci. USA* **99**, 10 765–10 770. (doi:10.1073/pnas.132272199)
17. Kida I, Rothman DL, Hyder F. 2007 Dynamics of changes in blood flow, volume, and oxygenation: implications for dynamic functional magnetic resonance imaging calibration. *J. Cereb. Blood Flow Metab.* **27**, 690–696. (doi:10.1038/sj.jcbfm.9600409)
18. Buxton RB, Uludaäÿ K, Dubowitz DJ, Liu TT. 2004 Modeling the hemodynamic response to brain activation. *Neuroimage* **23**, S220–S233. (doi:10.1016/j.neuroimage.2004.07.013)
19. Buzsaki G, Kaila K, Raichle M. 2007 Inhibition and brain work. *Neuron* **56**, 771–783. (doi:10.1016/j.neuron.2007.11.008)
20. Iadecola C. 2017 The neurovascular unit coming of age: a journey through neurovascular coupling in health and disease. *Neuron* **96**, 17–42. (doi:10.1016/j.neuron.2017.07.030)
21. Attwell D, Buchan AM, Charpak S, Lauritzen M, Macvicar BA, Newman EA. 2010 Glial and neuronal control of brain blood flow. *Nature* **468**, 232–243. (doi:10.1038/nature09613)
22. Logothetis NK. 2003 The underpinnings of the BOLD functional magnetic resonance imaging signal. *J. Neurosci.* **23**, 3963–3971. (doi:10.1523/JNEUROSCI.23-10-03963.2003)
23. Kim KJ, Ramiro Diaz J, Iddings JA, Filosa JA. 2016 Vasculo-neuronal coupling: retrograde vascular communication to brain neurons. *J. Neurosci.* **36**, 12 624–12 639. (doi:10.1523/JNEUROSCI.1300-16.2016)
24. Moore CI, Cao R. 2008 The hemo-neural hypothesis: on the role of blood flow in information processing. *J. Neurophysiol.* **99**, 2035–2047. (doi:10.1152/jn.01366.2006)
25. Sirotin YB, Das A. 2009 Anticipatory haemodynamic signals in sensory cortex not predicted by local neuronal activity. *Nature* **457**, 475–479. (doi:10.1038/nature07664)
26. Logothetis NK, Pauls J, Augath M, Trinath T, Oeltermann A. 2001 Neurophysiological investigation of the basis of the fMRI signal. *Nature* **412**, 150–157. (doi:10.1038/35084005)
27. Nir Y, Fisch L, Mukamel R, Gelbard-Sagiv H, Arieli A, Fried I, Malach R. 2007 Coupling between neuronal firing rate, gamma LFP, and BOLD fMRI is related to interneuronal correlations. *Curr. Biol.* **17**, 1275–1285. (doi:10.1016/j.cub.2007.06.066)
28. Mukamel R *et al.* 2005 Coupling between neuronal firing, field potentials, and fMRI in human auditory cortex. *Science* **309**, 951–954. (doi:10.1126/science.1110913)
29. Rees G, Friston K, Koch C. 2000 A direct quantitative relationship between the functional properties of human and macaque V5. *Nat. Neurosci.* **3**, 716–723. (doi:10.1038/76673)
30. Kim DS, Ronen I, Olman C, Kim S-G, Ugurbil K, Toth LJ. 2004 Spatial relationship between neuronal activity and BOLD functional MRI. *Neuroimage* **21**, 876–885. (doi:10.1016/j.neuroimage.2003.10.018)
31. Niessing J *et al.* 2005 Hemodynamic signals correlate tightly with synchronized gamma oscillations. *Science* **309**, 948–951. (doi:10.1126/science.1110948)
32. Logothetis NK. 2008 What we can do and what we cannot do with fMRI. *Nature* **453**, 869–878. (doi:10.1038/nature06976)
33. Attwell D, Laughlin SB. 2001 An energy budget for signaling in the grey matter of the brain. *J. Cereb. Blood Flow Metab.* **21**, 1133–1145. (doi:10.1097/00004647-200110000-00001)
34. Treves A, Rolls ET. 1991 What determines the capacity of autoassociative memories in the brain? *Network* **2**, 371–397. (doi:10.1088/0954-898X_2_4_004)
35. Harris KD, Henze DA, Csicsvari J, Hirase H, Buzsaki G. 2000 Accuracy of tetrode spike separation as determined by simultaneous intracellular and extracellular measurements. *J. Neurophysiol.* **84**, 401–414. (doi:10.1152/jn.2000.84.1.401)
36. Buzsaki G, Anastassiou CA, Koch C. 2012 The origin of extracellular fields and currents – EEG, ECoG, LFP and spikes. *Nat. Rev. Neurosci.* **13**, 407–420. (doi:10.1038/nrn3241)
37. Ray S, Maunsell JH. 2011 Different origins of gamma rhythm and high-gamma activity in macaque visual cortex. *PLoS Biol.* **9**, e1000610. (doi:10.1371/journal.pbio.1000610)
38. Lopes da Silva F. 2013 EEG and MEG: relevance to neuroscience. *Neuron* **80**, 1112–1128. (doi:10.1016/j.neuron.2013.10.017)
39. Niedermeyer E, Lopes da Silva F. 1999 *Electroencephalography: basic principles, clinical applications, and related fields*. Baltimore, MD: Lippincott Williams and Wilkins.
40. He BJ *et al.* 2008 Electrophysiological correlates of the brain's intrinsic large-scale functional architecture. *Proc. Natl Acad. Sci. USA* **105**, 16 039–16 044. (doi:10.1073/pnas.0807010105)
41. Crone NE, Sinai A, Korzeniewska A. 2006 High-frequency gamma oscillations and human brain mapping with electrocorticography. *Prog. Brain Res.* **159**, 275–295. (doi:10.1016/S0079-6123(06)59019-3)
42. Ray S, Crone NE, Niebur E, Franaszczuk PJ, Hsiao SS. 2008 Neural correlates of high-gamma oscillations (60–200 Hz) in macaque local field potentials and their potential implications in electrocorticography. *J. Neurosci.* **28**, 11 526–11 536. (doi:10.1523/JNEUROSCI.2848-08.2008)
43. Mitzdorf U. 1985 Current source-density method and application in cat cerebral cortex: investigation of evoked potentials and EEG phenomena. *Physiol. Rev.* **65**, 37–100. (doi:10.1152/physrev.1985.65.1.37)
44. Canolty RT, Edwards E, Dalal SS, Soltani M, Nagarajan SS, Kirsch HE, Berger MS, Barbaro NM, Knight RT. 2006 High gamma power is phase-locked to theta oscillations in human neocortex. *Science* **313**, 1626–1628. (doi:10.1126/science.1128115)
45. Ray S, Maunsell JH. 2010 Differences in gamma frequencies across visual cortex restrict their possible use in computation. *Neuron* **67**, 885–896. (doi:10.1016/j.neuron.2010.08.004)
46. Mountcastle VB. 1997 The columnar organization of the neocortex. *Brain* **120**, 701–722. (doi:10.1093/brain/120.4.701)
47. Penfield W, Boldrey E. 1937 Somatic motor and sensory representation in the cerebral cortex of man

as studied by electrical stimulation. *Brain* **60**, 389–443. (doi:10.1093/brain/60.4.389)

48. Henrie JA, Shapley R. 2005 LFP power spectra in V1 cortex: the graded effect of stimulus contrast. *J. Neurophysiol.* **94**, 479–490. (doi:10.1152/jn.00919.2004)
49. Nase G, Singer W, Monyer H, Engel AK. 2003 Features of neuronal synchrony in mouse visual cortex. *J. Neurophysiol.* **90**, 1115–1123. (doi:10.1152/jn.00480.2002)
50. Hermes D, Miller KJ, Vansteensel MJ, Aarnoutse EJ, Leijten FSS, Ramsey NF. 2012 Neurophysiologic correlates of fMRI in human motor cortex. *Hum. Brain Mapp.* **33**, 1689–1699. (doi:10.1002/hbm.21314)
51. Hubel DH, Wiesel TN. 1962 Receptive fields, binocular interaction and functional architecture in the cat's visual cortex. *J. Physiol.* **160**, 106–154. (doi:10.1113/jphysiol.1962.sp006837)
52. Buzsaki G, Moser EI. 2013 Memory, navigation and theta rhythm in the hippocampal–entorhinal system. *Nat. Neurosci.* **16**, 130–138. (doi:10.1038/nn.3304)
53. Redish AD, Rosenzweig ES, Bohanick JD, Mcnaughton BL, Barnes CA. 2000 Dynamics of hippocampal ensemble activity realignment: time versus space. *J. Neurosci.* **20**, 9298–9309. (doi:10.1523/JNEUROSCI.20-24-09298.2000)
54. Pare D, Decurtis M, Llinas R. 1992 Role of the hippocampal–entorhinal loop in temporal lobe epilepsy: extra-and intracellular study in the isolated guinea pig brain in vitro. *J. Neurosci.* **12**, 1867–1881. (doi:10.1523/JNEUROSCI.12-05-01867.1992)
55. Yamaguchi Y. 2003 A theory of hippocampal memory based on theta phase precession. *Biol. Cybern.* **89**, 1–9. (doi:10.1007/s00422-003-0415-9)
56. Ekstrom A, Suthana N, Millett D, Fried I, Bookheimer S. 2009 Correlation between BOLD fMRI and theta-band local field potentials in the human hippocampal area. *J. Neurophysiol.* **101**, 2668–2678. (doi:10.1152/jn.91252.2008)
57. Carmichael DW, Thornton JS, Rodionov R, Thornton R, Mcevoy AW, Ordidge RJ, Allen PJ, Lemieux L. 2009 Feasibility of simultaneous intracranial EEG-fMRI in humans: a safety study. *Neuroimage* **49**, 379–390. (doi:10.1016/j.neuroimage.2009.07.062)
58. Miezin FM, Maccotta L, Ollinger JM, Petersen SE, Buckner RL. 2000 Characterizing the hemodynamic response: effects of presentation rate, sampling procedure, and the possibility of ordering brain activity based on relative timing. *Neuroimage* **11**, 735–759. (doi:10.1006/nimg.2000.0568)
59. Shmuel A, Augath M, Oeltermann A, Logothetis NK. 2006 Negative functional MRI response correlates with decreases in neuronal activity in monkey visual area V1. *Nat. Neurosci.* **9**, 569–577. (doi:10.1038/nn1675)
60. Goense JB, Logothetis NK. 2008 Neurophysiology of the BOLD fMRI signal in awake monkeys. *Curr. Biol.* **18**, 631–640. (doi:10.1016/j.cub.2008.03.054)
61. Huttunen JK *et al.* 2008 Coupling between simultaneously recorded BOLD response and neuronal activity in the rat somatosensory cortex. *Neuroimage* **39**, 775–785. (doi:10.1016/j.neuroimage.2007.06.042)
62. Ureshi M, Matsuura T, Kanno I. 2004 Stimulus frequency dependence of the linear relationship between local cerebral blood flow and field potential evoked by activation of rat somatosensory cortex. *Neurosci. Res.* **48**, 147–153. (doi:10.1016/j.neures.2003.10.014)
63. Parvizi J, Kastner S. 2018 Promises and limitations of human intracranial electroencephalography. *Nat. Neurosci.* **21**, 474. (doi:10.1038/s41593-018-0108-2)
64. Rauch A, Rainer G, Logothetis NK. 2008 The effect of a serotonin-induced dissociation between spiking and perisynaptic activity on BOLD functional MRI. *Proc. Natl Acad. Sci. USA* **105**, 6759–6764. (doi:10.1073/pnas.0800312105)
65. Viswanathan A, Freeman RD. 2007 Neurometabolic coupling in cerebral cortex reflects synaptic more than spiking activity. *Nat. Neurosci.* **10**, 1308–1312. (doi:10.1038/nn1977)
66. Lauritzen M, Gold L. 2003 Brain function and neurophysiological correlates of signals used in functional neuroimaging. *J. Neurosci.* **23**, 3972–3980. (doi:10.1523/JNEUROSCI.23-10-03972.2003)
67. Kucyi A *et al.* 2020 Electrophysiological dynamics of antagonistic brain networks reflect attentional fluctuations. *Nat. Commun.* **11**, 325. (doi:10.1038/s41467-019-14166-2)
68. Ekstrom A, Viskontas I, Kahana M, Jacobs J, Upchurch K, Bookheimer S, Fried I. 2007 Contrasting roles of neural firing rate and local field potentials in human memory. *Hippocampus* **17**, 606–617. (doi:10.1002/hipo.20300)
69. Li B, Gong L, Wu R, Li A, Xu F. 2014 Complex relationship between BOLD-fMRI and electrophysiological signals in different olfactory bulb layers. *Neuroimage* **95**, 29–38. (doi:10.1016/j.neuroimage.2014.03.052)
70. Herman P, Sanganahalli BG, Blumenfeld H, Rothman DL, Hyder F. 2013 Quantitative basis for neuroimaging of cortical laminae with calibrated functional MRI. *Proc. Natl Acad. Sci. USA* **110**, 15 115–15 120. (doi:10.1073/pnas.1307154110)
71. Conner CR, Ellmore TM, Pieters TA, Disano MA, Tandon N. 2011 Variability of the relationship between electrophysiology and BOLD-fMRI across cortical regions in humans. *J. Neurosci.* **31**, 12 855–12 865. (doi:10.1523/JNEUROSCI.1457-11.2011)
72. Kujala J *et al.* 2014 Multivariate analysis of correlation between electrophysiological and hemodynamic responses during cognitive processing. *Neuroimage* **92**, 207–216. (doi:10.1016/j.neuroimage.2014.01.057)
73. Schridde U, Khubchandani M, Motelow JE, Sanganahalli BG, Hyder F, Blumenfeld H. 2008 Negative BOLD with large increases in neuronal activity. *Cereb. Cortex* **18**, 1814–1827. (doi:10.1093/cercor/bhm208)
74. Englot DJ, Mishra AM, Mansuripur PK, Herman P, Hyder F, Blumenfeld H. 2008 Remote effects of focal hippocampal seizures on the rat neocortex. *J. Neurosci.* **28**, 9066–9081. (doi:10.1523/JNEUROSCI.2014-08.2008)
75. Borowsky IW, Collins RC. 1989 Metabolic anatomy of brain: a comparison of regional capillary density, glucose metabolism, and enzyme activities. *J. Comp. Neurol.* **288**, 401–413. (doi:10.1002/cne.902880304)
76. Shaw K, Bell L, Boyd K, Grijseels DM, Clarke D, Bonnar O, Crombag HS, Hall CN. 2019 Hippocampus has lower oxygenation and weaker control of brain blood flow than cortex, due to microvascular differences. *bioRxiv*, 835728. (doi:10.1101/835728)
77. Ances BM, Leontiev O, Perthen JE, Liang C, Lansing AE, Buxton RB. 2008 Regional differences in the coupling of cerebral blood flow and oxygen metabolism changes in response to activation: implications for BOLD-fMRI. *Neuroimage* **39**, 1510–1521. (doi:10.1016/j.neuroimage.2007.11.015)
78. O'Keefe J, Dostrovsky J. 1971 The hippocampus as a spatial map. Preliminary evidence from unit activity in the freely-moving rat. *Brain Res.* **34**, 171–175. (doi:10.1016/0006-8993(71)90358-1)
79. Wilson MA, McNaughton BL. 1993 Dynamics of the hippocampal ensemble code for space. *Science* **261**, 1055–1058. (doi:10.1126/science.8351520)
80. Redish AD *et al.* 2001 Independence of firing correlates of anatomically proximate hippocampal pyramidal cells. *J. Neurosci.* **21**, RC134. (doi:10.1523/JNEUROSCI.21-05-j0004.2001)
81. Nolan CR, Vromen JMG, Cheung A, Baumann O. 2018 Evidence against the detectability of a hippocampal place code using functional magnetic resonance imaging. *eNeuro* **5**, ENEURO.0177-18.2018. (doi:10.1523/ENEURO.0177-18.2018)
82. Yacoub E, Harel N, Ugurbil K. 2008 High-field fMRI unveils orientation columns in humans. *Proc. Natl Acad. Sci. USA* **105**, 10 607–10 612. (doi:10.1073/pnas.0804110105)
83. Kamitani Y, Tong F. 2005 Decoding the visual and subjective contents of the human brain. *Nat. Neurosci.* **8**, 679–685. (doi:10.1038/nn1444)
84. Dubois J, De Berker AO, Tsao DY. 2015 Single-unit recordings in the macaque face patch system reveal limitations of fMRI MVPA. *J. Neurosci.* **35**, 2791–2802. (doi:10.1523/JNEUROSCI.4037-14.2015)
85. Ekstrom AD, Harootonian SK, Huffman DJ. 2019 Grid coding, spatial representation, and navigation: should we assume an isomorphism? *Hippocampus* **30**, 422–432. (doi:10.1002/hipo.23175)
86. Mukamel R, Fried I. 2012 Human intracranial recordings and cognitive neuroscience. *Annu. Rev. Psychol.* **63**, 511–537. (doi:10.1146/annurev-psych-120709-145401)
87. Ollinger J, Shulman GL, Corbetta M. 2001 Separating processes within a trial in event-related functional MRI: I. The method. *Neuroimage* **13**, 210–217. (doi:10.1006/nimg.2000.0710)
88. Hermes D, Nguyen M, Winawer J. 2017 Neuronal synchrony and the relation between the blood-oxygen-level dependent response and the local field potential. *PLoS Biol.* **15**, e2001461. (doi:10.1371/journal.pbio.2001461)
89. Mathiesen C, Caesar K, Lauritzen M. 2000 Temporal coupling between neuronal activity and blood flow

in rat cerebellar cortex as indicated by field potential analysis. *J. Physiol.* **523**, 235–246. (doi:10.1111/j.1469-7793.2000.t01-1-00235.x)

90. Haxby JV *et al.* 2001 Distributed and overlapping representations of faces and objects in ventral temporal cortex. *Science* **293**, 2425–2430. (doi:10.1126/science.1063736)
91. Kriegeskorte N, Bandettini P. 2007 Analyzing for information, not activation, to exploit high-resolution fMRI. *Neuroimage* **38**, 649–662. (doi:10.1016/j.neuroimage.2007.02.022)
92. Hanke M *et al.* 2009 PyMVPA: a unifying approach to the analysis of neuroscientific data. *Front. Neuroinform.* **3**, 3. (doi:10.3389/neuro.11.003.2009)
93. Norman KA, Polyn SM, Detre GJ, Haxby JV. 2006 Beyond mind-reading: multi-voxel pattern analysis of fMRI data. *Trends Cogn. Sci.* **10**, 424–430. (doi:10.1016/j.tics.2006.07.005)
94. Polyn SM, Norman KA, Kahana MJ. 2009 A context maintenance and retrieval model of organizational processes in free recall. *Psychol. Rev.* **116**, 129–156. (doi:10.1037/a0014420)
95. Komorowski RW, Garcia CG, Wilson A, Hattori S, Howard MW, Eichenbaum H. 2013 Ventral hippocampal neurons are shaped by experience to represent behaviorally relevant contexts. *J. Neurosci.* **33**, 8079–8087. (doi:10.1523/JNEUROSCI.5458-12.2013)
96. Farovik A, Place RJ, Mckenzie S, Porter B, Munro CE, Eichenbaum H. 2015 Orbitofrontal cortex encodes memories within value-based schemas and represents contexts that guide memory retrieval. *J. Neurosci.* **35**, 8333–8344. (doi:10.1523/JNEUROSCI.0134-15.2015)
97. Copara MS, Hassan AS, Kyle CT, Libby LA, Ranganath C, Ekstrom AD. 2014 Complementary roles of human hippocampal subregions during retrieval of spatiotemporal context. *J. Neurosci.* **34**, 6834–6842. (doi:10.1523/JNEUROSCI.5341-13.2014)
98. Huffman DJ, Ekstrom AD. 2019 A modality-independent network underlies the retrieval of large-scale spatial environments in the human brain. *Neuron* **104**, 611–622.e7. (doi:10.1016/j.neuron.2019.08.01)
99. Lindquist MA, Meng Loh J, Atlas LY, Wager TD. 2009 Modeling the hemodynamic response function in fMRI: efficiency, bias and mis-modeling. *Neuroimage* **45**, S187–S198. (doi:10.1016/j.neuroimage.2008.10.065)
100. Eklund A, Nichols TE, Knutsson H. 2016 Cluster failure: why fMRI inferences for spatial extent have inflated false-positive rates. *Proc. Natl Acad. Sci. USA* **113**, 7900–7905. (doi:10.1073/pnas.1602413113)
101. Saad ZS, Ropella KM, Deyoe EA, Bandettini PA. 2003 The spatial extent of the BOLD response. *Neuroimage* **19**, 132–144. (doi:10.1016/S1053-8119(03)00016-8)
102. Lachaux JP, Rudrauf D, Kahane P. 2003 Intracranial EEG and human brain mapping. *J. Physiol. Paris* **97**, 613–628. (doi:10.1016/j.jphysparis.2004.01.018)
103. Wardle SG, Kriegeskorte N, Grootswagers T, Khaligh-Razavi S-M, Carlson TA. 2016 Perceptual similarity of visual patterns predicts dynamic neural activation patterns measured with MEG. *Neuroimage* **132**, 59–70. (doi:10.1016/j.neuroimage.2016.02.019)
104. Serences JT, Ester EF, Vogel EK, Awh E. 2009 Stimulus-specific delay activity in human primary visual cortex. *Psychol. Sci.* **20**, 207–214. (doi:10.1111/j.1467-9280.2009.02276.x)
105. Kriegeskorte N, Mur M, Ruff DA, Kiani R, Bodurka J, Esteky H, Tanaka K, Bandettini PA. 2008 Matching categorical object representations in inferior temporal cortex of man and monkey. *Neuron* **60**, 1126–1141. (doi:10.1016/j.neuron.2008.10.043)
106. Kriegeskorte N. 2009 Relating population-code representations between man, monkey, and computational models. *Front. Neurosci.* **3**, 35. (doi:10.3389/neuro.01.035.2009)